HETEROCYCLES, Vol. 104, No. 5, 2022, pp. 979 - 986. © 2022 The Japan Institute of Heterocyclic Chemistry
Received, 6th January, 2022, Accepted, 2nd February, 2022, Published online, 10th February, 2022
DOI: 10.3987/COM-22-14623

SYNTHESIS OF COVALENT BOROXINE FRAMEWORKS BY POLYCONDENSATION OF TETRAHYDROXYDIBORON

Haruka Yamauchi,[a] Atsushi Asano,[b] and Shotaro Hayashi[a,c]*

a School of Environmental Science and Engineering, Kochi University of Technology, 185 Tosayamada Miyanokuchi, Kami, Kochi, 782-8502, Japan.
b Department of Applied Chemistry, National Defense Academy, 1-10-20 Hashirimizu, Yokosuka, 239-8686, Japan.
c Research Center for Molecular Design, Kochi University of Technology. E-mail: hayashi.shotaro@kochi-tech.ac.jp

Abstract – We have demonstrated synthesis of boroxine networks by condensation of tetrahydroxydiboron. The network material was obtained in quantitative yield by microwave-assisted heating of *N*,*N*-dimethylacetamide. The material had a crystalline structure and good stability. In addition, the material could be easily decomposed to the monomer by water addition.

Various frameworks have recently attracted much attention because of their potential applications.[1] Metal–organic frameworks are a class of compounds consisting of metal ions coordinated to pillar organic ligands to form zero- to three-dimensional structures.[2] The combination of metals and ligands can be arranged to produce frameworks with different porosity, functionality, and shape.[2] Frameworks based on intermolecular interactions are also interesting and useful materials.[3] Porous molecular crystals have attracted much attention, including hydrogen-bonded organic frameworks,[3a] supramolecular organic frameworks,[3b] and porous organic salts.[3c] Covalent organic frameworks (COFs) have also been widely studied as two- or three-dimensional materials, in which the building blocks are linked by strong covalent bonds.[4] Facile synthesis by polycondensation allows relatively easy access to the frameworks. Boron condensation of phenylenediboronic acid is the most popular route to synthesize COFs.[5] In this case, three boronic acid groups converge to form a planar six-membered boroxine ring through elimination of water. Not only can various arylboronic acids be used for COF synthesis, but the porosity and function can be controlled by their organic structure. However, there have been no reports of condensation of tetrahydroxydiboron, which could possibly give covalently bonded frameworks based on two elements (B and O). For synthesis of frameworks that do not contain organic structures, using tetrahydroxydiboron as a

monomer is considered to be effective for synthesis of COFs containing B–B bonds. Herein, we report synthesis of covalent boroxine framework (**CBOF**s) and their properties.

Readily available tetrahydroxydiboron (TCI Co.) was used as the monomer for polycondensation synthesis of the **CBOF** (Scheme 1). However, the **CBOF** was not obtained by heating tetrahydroxydiboron (**THB**) at various temperatures (100–150 °C) for 1 day in methylene-dioxane or dioxane solution in a sealed tube (Table 1, entries 1–6). These conditions have typically been used for COF synthesis from aryldiboronic acids, such as phenylene-1,4-diboronic acid.[5] A more polar solvent system is required because the low solubility of **THB** in methylene-dioxane prevents condensation. Condensation at 150 °C in dry *N*,*N*-dimethylacetamide (DMAc) for 3 h gave a white precipitate. The precipitate was washed with DMAc and dichloromethane to give a white powder (**CBOF1**) in low yield (<10%) (Table 1, entries 7 and 8). Interestingly, microwave-assisted polycondensation (150 °C, 30 min, Monowave, Anton Paar) in DMAc gave a large-scale white glassy solid (**CBOF2**) in quantitative yield (Table 1, entries 9 and 10). This may be because of the solubility of **THB** in DMAc and the fast heating rate or overshoot in the initial stage of microwave heating (Figure S1).

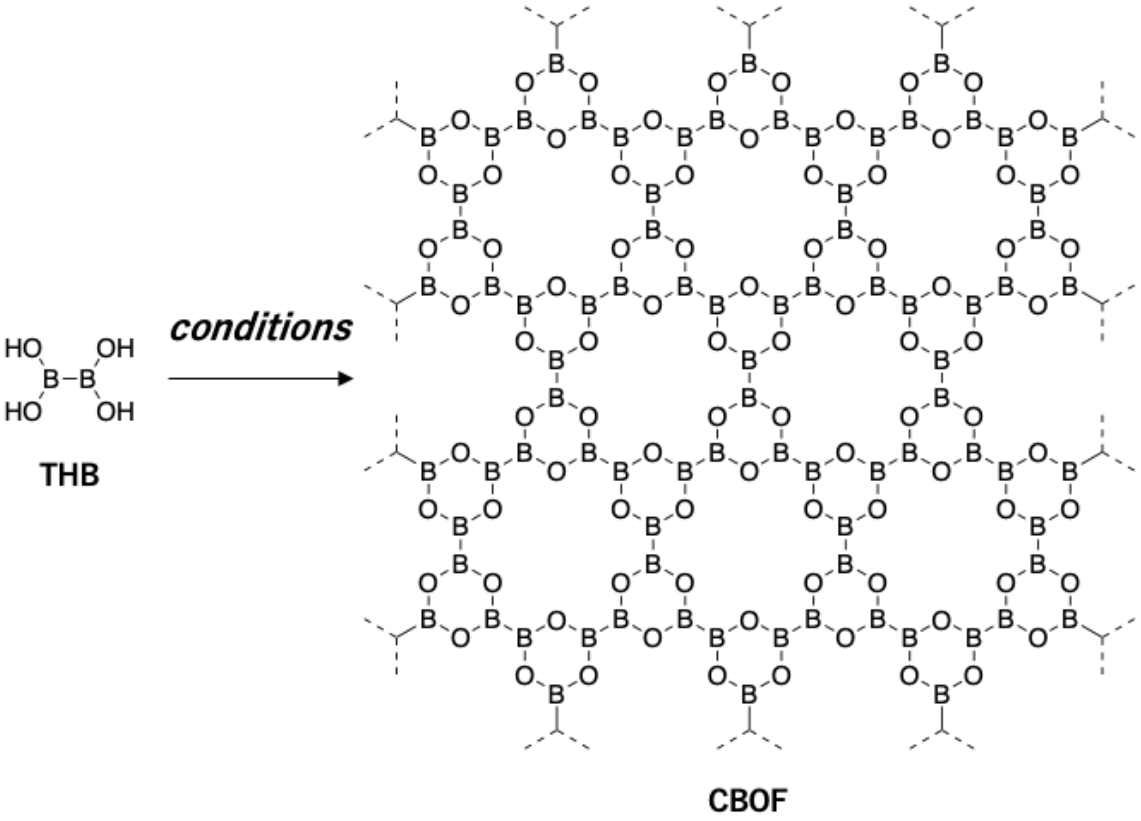

Scheme 1. Synthesis of the **CBOF** by polycondensation of **THB**. The detailed conditions are given below Table 1.

Table 1. Condensation results

Entry	Solvents	Heating (Temp., °C/ Time, h)	Yield, %
1	methytylene-dioxane	oil bath [a] (100/24)	- [b]
2	methytylene-dioxane	oil bath [a] (130/24)	- [b]
3	methytylene-dioxane	oil bath [a] (150/24)	- [b]
4	dioxane	oil bath [a] (100/24)	- [b]
5	dioxane	oil bath [a] (130/24)	- [b]
6	dioxane	oil bath [a] (150/24)	- [b]
7	DMAc	oil bath [a] (100/24)	trace
8	DMAc	oil bath [a] (150/24)	10
9	DMAc	microwave (150/1)	quant.
10	DMAc	microwave (150/0.5)	quant.

Conditions: sealed reaction tube, **THB** (2.0 mmol), solvent (1 mL), specified temperature/time. [a]The reaction tube was heated in an oil bath at a preset temperature. [b]A solid was not obtained.

To investigate the structure of the obtained insoluble material **CBOF2**, the solid-state ^{11}B magic-angle-spinning (MAS) NMR spectrum was measured (Figure 1a). Because boron has a quadrupole nucleus (spin I is 3/2), the signal of the NMR spectrum becomes complicated and it has an asymmetric line shape owing to the interaction between the electric field gradient tensor and the quadrupole moment of boron. The present ^{11}B MAS NMR spectrum of **THB** was comparable with a previously measured spectrum.[6] The obtained material from condensation of **THB** (**CBOF2**) showed a similar ^{11}B MAS NMR signal to that of borax (Figure S3).[7] The asymmetric signal consisting of two peaks at 5 and 14 ppm is ascribed to three-coordinated boron (B3). The strong and sharp symmetric peak at 0.67 ppm is four-coordinated boron (B4). This site has a very weak quadrupolar interaction, so that the signal becomes symmetric and has a narrow line shape. This indicates that the eliminated H_2O was slightly coordinated to B–B under the DMAc weakly basic condition. Furthermore, the ^{11}B MAS NMR spectrum of **CBOF2** included the remaining **THB** or **CBOF2** had a similar structure to **THB**, because the small shoulder signals at around −3 and 15.6 ppm come from the same origin, a boron site like in **THB**.

Structural characterization was carried out by powder X-ray diffraction (PXRD). The experimental pattern of **CBOF2** was compared with the pattern of **CBOF1** (Figure 2a). For **CBOF1**, only a very fuzzy pattern was observed, but a broad yet clear peak was observed for **CBOF2**. The synthetic method resulted in significantly different crystallinity. Although both **CBOF**s were found to also contain amorphous segments, well-defined short-range order was observed, which corresponds to some theoretically expected pore sizes (Figure 2b). Structural optimisations were performed by density functional theory (DFT, Gaussian, B3LYP/6-31G level). During the calculations, the **CBOF** structures were optimised from completely planar two-dimensional sheets to nonplanar configurations, exhibiting torsion within the B–B bonds in the frameworks (Figure 2c). This suggests that the framework near the central part was twisted, and holes with a planar structure formed toward the outside. Since it is estimated that it forms a 3D structure with various B-B twisted angles, this theoretical sheet structure does not completely fit in PXRD patterns (Figure 2a). Thus, the variety of patterns determined from various PXRD (4.27-8.88 Å) peaks is different from the ring size (6.3 Å) of the DFT optimized structure. This is consistent with detection of multiple random crystalline patterns without a uniform pore skeleton throughout the framework.

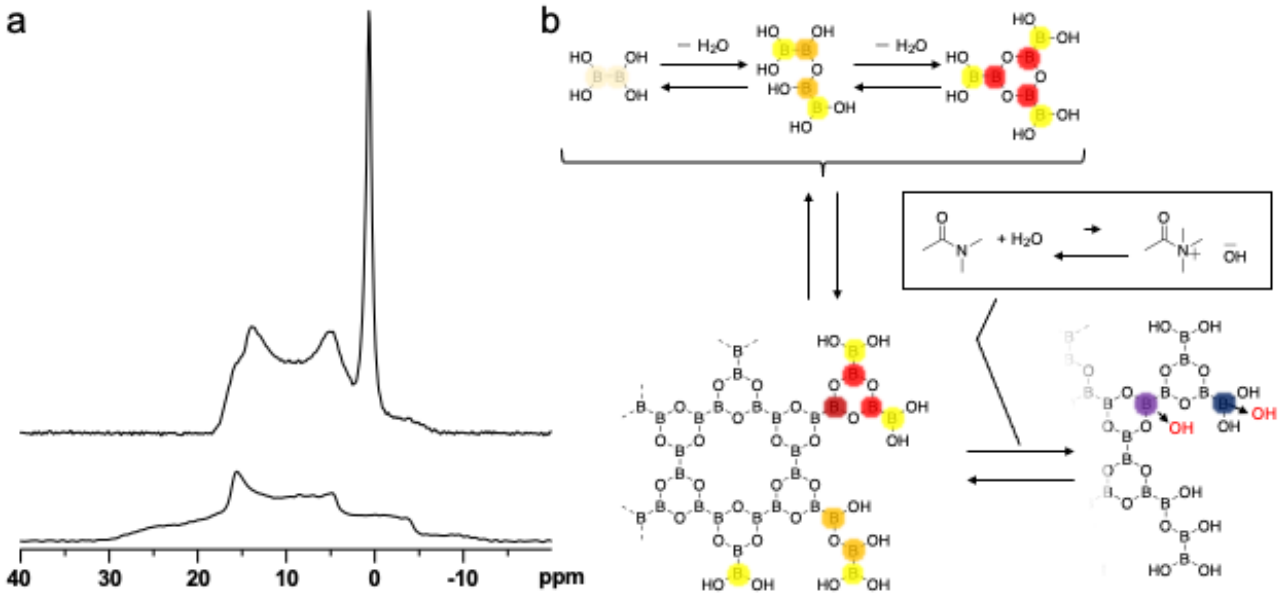

Figure 1. (a) Solid-state ^{11}B MAS NMR spectra of **CBOF2** (top) and **THB** (bottom) at 9.4 T magnetic field and MAS rate of 12.5 kHz. The ^{11}B chemical shift of $NaBH_4$ at −42.06 ppm was used as an external reference. (b) Structure and condensation process of **THB**.

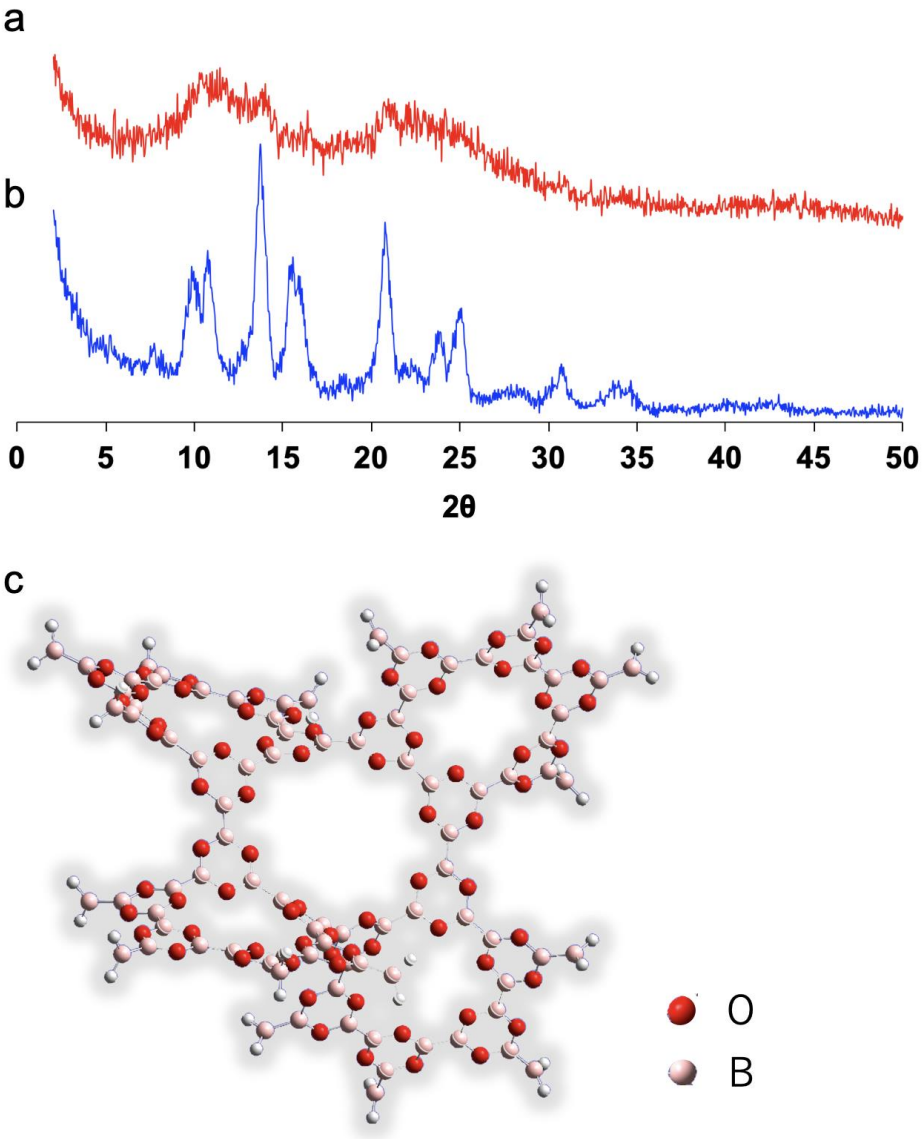

Figure 2. (a) PXRD pattern of **CBOF1**. (b) PXRD pattern of **CBOF2**. (c) DFT-simulated structure of fragmentated **CBOF**. Red: oxygen. Pink: boron. White: hydrogen.

The infrared (IR) spectra of the CBOFs were recorded to investigate the specific functional groups (Figures S4–S6). The spectra of **CBOF**s show a slight absorption band at 3200-3300 cm^{-1} similar to the spectrum of **THB**. These results support the existence of the residual hydroxy group. We suspected the presence of the solvent (DMAc) in the network structure, but no strong stretching vibrations (ca. 1650 cm^{-1}) from the amide group of DMAc were observed in the IR spectra. Therefore, DMAc, which is supposed to be an impurity, was not detected.

Thermogravimetric analysis (TGA) and differential thermal analysis (DTA) were performed to investigate not only the thermal properties, but also the reaction of the materials (Figure S7). Two endothermic peaks (140 and 160 °C) were observed for **THB**. This is considered to be because of vaporisation of water because **THB** melting and condensation immediately occurred. The weight loss shown by TGA also suggested

progression of dehydration. Conversely, for **CBOF1**, it is presumed that condensation and dehydration of the part where the water adsorbed on the powder surface desorbed from the surface occurred in the range 200–240 °C. Boroxine formation from unreacted boronic acid then probably occurred (>240 °C). A gradual weight decrease of **CBOF2** was observed from around 150 °C, although no clear DTA peak was observed. It is also presumed that evaporation of water adsorbed on the surface occurred. Condensation of the unreacted boronic acid progressed above 240 °C. It is considered that desorption of adsorbed water is affected by the hydrophilicity of the material. It is presumed that **CBOF2**, in which condensation effectively occurs, has a low surface adsorption ability for water. The results may depend on the number of surface-facing functional groups, especially boronic acid groups, but further investigation is required. To investigate that no structural transition occurred in this process, XRD measurement of **CBOF2** before and after heating at 240 °C was performed (Figure S8). These results indicate that the crystallinity of **CBOF2** has not changed due to heating.

Macroscopic and scanning electron microscopy (SEM) images of **CBOF1** and **CBOF2** are shown in Figure 3. **CBOF2** was larger than **CBOF1** (Figures 3a and c). No clear difference in the morphologies of the two **CBOF**s was observed, but the surface of **CBOF2** was rough (Figures 3b and d). To quantify the porosity levels, nitrogen-gas sorption measurements were performed (Figure S9a). The isotherm slightly increased in the low relative pressure region and greatly increased in the high-pressure region. The isotherm of **CBOF2** resembled a typical type II isotherm, indicating the presence of few micropores. Macropores did not exist because no large holes were observed in the SEM images. The surface area of **CBOF2** was calculated by Brunauer–Emmett–Teller (BET) theory. **CBOF2** exhibited a poor porosity level, with a BET surface area of 0.48 $m^2\ g^{-1}$. The pore-size distribution showed that **CBOF2** possessed a narrow pore-size distribution with an average pore size of 5.1 nm (Figure S9b), corresponding to the micropores of the framework. A low BET specific surface indicates that micropores and micropores are almost not contained in the **CBOF** solid, and a THB-derived network structure with a dense solid structure formed.

The **CBOF**s did not dissolve in organic solvents, but they decomposed when alcohols were added. Addition of water also decomposed the **CBOF**s, giving the **THB** monomer. When water was added to bulk **CBOF2** (50 mg) and left to stand, it completely decomposed in about 2 min (Figure 3e). Thus, the **CBOF**s are recyclable materials that can be decomposed and returned to **THB**.

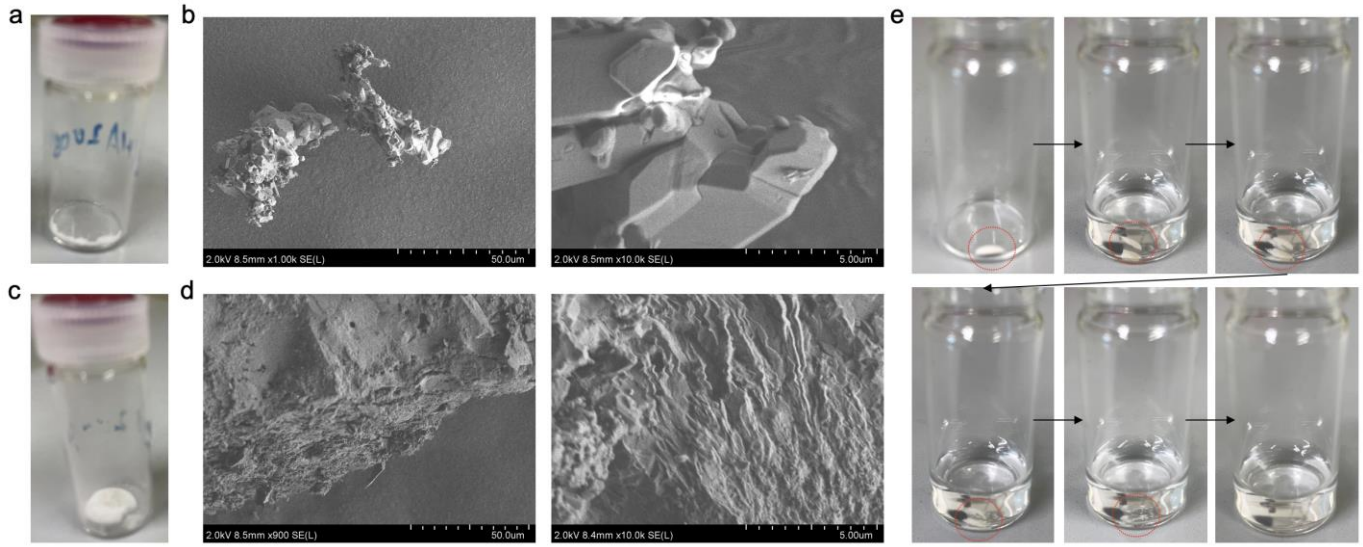

Figure 3. (a) Photograph and (b) SEM images of **CBOF1**. (c) Photograph and (d) SEM images of **CBOF2**. (e) Decomposition of **CBOF2** by addition of water.

In summary, we have reported synthesis of a framework consisting only of boroxine by condensation of tetrahydroxydiboron. The highly water-soluble monomer was efficiently condensed by microwave heating in a highly polar solvent to obtain a crystalline framework material. Although it showed good stability to heat and organic solvents, it could be decomposed with water and alcohols. When water was added to the bulk material, it decomposed in just a few minutes. Not only can tetrahydroxydiboron be used to synthezise inorganic frameworks consisting of boroxine, COFs containing diboron could also be realised by combining tetrahydroxydiboron with various monomers.

EXPERIMENTAL

Synthesis. Microwave-assisted heating was performed using Discover (CEM) and Monowave (Anton Paar). The reaction vessel was a dedicated 10 mL glass vessel, the reaction was carried out in a closed system, and the temperature was measured at any time with the attached IR sensor. Tetrahydroxydiboron (TCI co. 90 mg, 10 mmol) and DMAc (Wako, 1 mL) was added to reaction tube, then heated to 150 °C. for 30 min. Obtained solid was washed with DMAc and CH_2Cl_2.

Measurements. Solid-state ^{11}B magic-angle spinning (MAS) NMR spectrum was measured using a Varian NMR systems 400WB spectrometer with MAS rate of 12.5 kHz and ^{1}H high power TPPM decoupling of 108 kHz. The 90º pulse length of 0.8 μs was used. The specific surface areas of the samples were measured by N_2 gas adsorption at 77 K using an automated adsorption apparatus (BELSORP-max, BEL Japan Inc.). The system and sample were outgassed at 293 K for 6 h to obtain a residual pressure of $<10^{-4}$ Pa prior to the adsorption experiments. IR measurement was performed by a Jasco FT/IT-480 Plus spectrometer. SEM images were taken on a Hitachi SU8020 microscope. TGA analysis was performed by a Hitachi

STA7200RV, which measured during heating from room temperature to 600 °C at heating rate of 20 °C/min in nitrogen.

ACKNOWLEDGEMENTS

S. H. acknowledges funding from KAKENHI (Grant-in-Aid for Scientific Research B, no. 18H02052, Grant-in-Aid for Scientific Research on Innovative Areas "π-Figuration") of the Japan Society for the Promotion of Science (JSPS). We thank Edanz (https://jp.edanz.com/ac) for editing a draft of this manuscript.

REFERENCES

1. (a) T. Liu and G. Liu, *Nat. Commun.*, 2020, **11**, 4984; (b) T. D. Bennett, F.-X. Coudert, S. L. James, and A. I. Cooper, *Nat. Mater.*, 2021, **20**, 1179; (c) J. Yu, A. Corma, and Y. Li, *Adv. Mater.*, 2020, 2006277; (d) S. Hayashi, S. Yamamoto, K. Nishi, A. Asano, and T. Koizumi, *Polym. J.*, 2019, **51**, 1055; (e) S. Hayashi, Y. Togawa, S. Yamamoto, T. Koizumi, K. Nishi, and A. Asano, *J. Polym. Sci. Part A: Polym. Chem.*, 2017, **55**, 3862.
2. (a) R.-B, Lin, S. Xiang, W. Zhou, and B. Chen, *Chem.*, 2020, **6**, 337; (b) Y.-S. Wei, M. Zhang, R. Zou, and Q. Xu, *Chem. Rev.*, 2020, **120**, 12089; (c) K. Geng, T. He, R. Liu, S. Dalapati, K. T. Tan, Z. Li, S. Tao, Y. Gong, Q. Jiang, and D. Jiang, *Chem. Rev.*, 2020, **120**, 8814; (d) Y. Tian and G. Zhu, *Chem. Rev.*, 2020, **120**, 8934; (e) G. Bian, J. Yin, and J. Zhu, *Small*, 2021, **17**, 2006043; (f) L. Yu, Z.-B. Li, and D. Wang, *Chem. Commun.*, 2016, **52**, 13771.
3. (a) I. Hisaki, *J. Incl. Phenom. Macro. Chem.*, 2020, **96**, 215; (b) W. Yang, A. Greenaway, X. Lin, R. Matsuda, A. J. Blake, C. Wilson, W. Lewis, P. Hubberstey, S. Kitagawa, N. R. Champness, and M. Schröder, *J. Am. Chem. Soc.*, 2010, **132**, 14457; (c) A. Yamamoto, S. Uehara, T. Hamada, M. Miyata, I. Hisaki, and N. Tohnai, *Cryst. Growth Des.*, 2012, **12**, 4600.
4. (a) P. J. Waller, F. Gándara, and O. M. Yaghi, *Acc. Chem. Res.*, 2015, **48**, 3053; (b) C. S. Diercks, and O. M. Yaghi, *Science*, 2017, **355**, eaal1585; (c) X. Feng, X. Ding, and D. Jiang, *Chem. Soc. Rev.*, 2012, **41**, 6010.
5. (a) A. P. Côté, A. I. Benin, N. W. Ockwig, M. O'Keeffe, A. J. Matzger, and O. M. Yaghi, *Science*, 2005, **310**, 1166; (b) S. B. Kalidindi, C. Wiktor, A. Ramakrishnan, J. Weßing, A. Schneemann, G. V. Tendeloo, and R. A. Fischer, *Chem. Commun.*, **49**, 463.
6. F. A. Perras and D. L. Bryce, *Chem. Sci.*, 2014, **5**, 2428.
7. K. Yamada, in *ACS Symposium Series* Vol. 1077; NMR Spectroscopy of Polymers: Innovative NMR Strategies for Complex Macromolecular Systems, ed. by H. N. Cheng, T. Asakura, and A. D. English, Amer. Chem. Soc., Washington, DC, 2011, Ch. 8, pp.133.